JOURNAL OF MATERIALS SCIENCE 20 (1985) 2141–2147

The effect of hydrostatic pressure on the tensile properties of pultruded CFRP

T. V. PARRY, A. S. WRONSKI
School of Materials Science, University of Bradford, West Yorkshire, UK

The failure process in waisted tensile specimens of pultruded 60% volume fraction carbon fibre–epoxide was investigated at atmospheric and superposed hydrostatic pressures up to 300 MN m^{-2}. The maximum principal stress at fracture decreased from ~ 2.0 GN m^{-2} at atmospheric pressure to ~ 1.5 GN m^{-2} by 200 MN m^{-2} superposed pressure and then remained approximately constant. These latter failures were fairly flat and no damage preceding the catastrophic fracture was detected, which indicates that composite strength is solely controlled by fibre strength. Fracture of fibres at lower pressures appeared to commence also in the range 1.5 to 1.6 GN m^{-2}, but, as it did not result in catastrophic failure, account has to be taken of the resin and the fibre bundles. Debonding was initiated at ~ 1.2 GN m^{-2} at atmospheric pressure and this stress increased to ~ 1.5 GN m^{-2} when 150 MN m^{-2} superposed pressure was applied; the pressure dependence was related to that of the resin tensile strength. This process is described as the first stage, straightening and debond initiation of curved surface bundles, on our model of tensile failure. The second stage, delamination, i.e. the growth of transverse cracks leading to the detachment of these bundles, was impeded by the transverse pressure, being suppressed beyond 150 MN m^{-2}. Only below this pressure was load redistribution between bundles possible, but, as the pressure was increased from atmospheric, it become more difficult, resulting in a decrease in the composite tensile strength and reduced fibre pull-out.

1. Introduction

It is generally accepted that the tensile strength of unidirectionally aligned continuous fibrous composites is determined by the breaking strength of the fibres [1–6]. Detailed theories of composite strength have thus recently tended to analyse acoustic activity [2, 3] and statistical strength distributions of fibres [3]. A typical argument suggests that, if the matrix has been well chosen, the fibres will reach their breaking strain before the matrix fails and its role is to isolate fibre breaks in a narrow section of the composite due to load transfer into the fibre produced by shear deformation of the matrix, as described by Rosen [6]. It should be pointed out, however, that Rosen's elegant experiments were on 6% volume fraction, V_f, of glass-reinforced plastic lamina of ~ 100 fibres, hardly a high strength composite.

Recently [7] we have examined the microstructures of pultruded 60% V_f carbon fibre reinforced epoxide, CFRP, strained in tension and suggested a three-stage failure process: (a) "initiation": the straightening and debonding of misaligned surface fibre bundles; (b) "growth": the detachment of these bundles through the growth of transverse cracks and (c) "propagation" of failure through the fracture of fibre bundles (typically tows) at various cross-sections. Application of hydrostatic pressure, H, to the tensile testing stress system is a good test of the model, as H effects differently shear and tensile stress-operated mechanisms. In particular a critical

0022–2461/85 $03.00 + .12

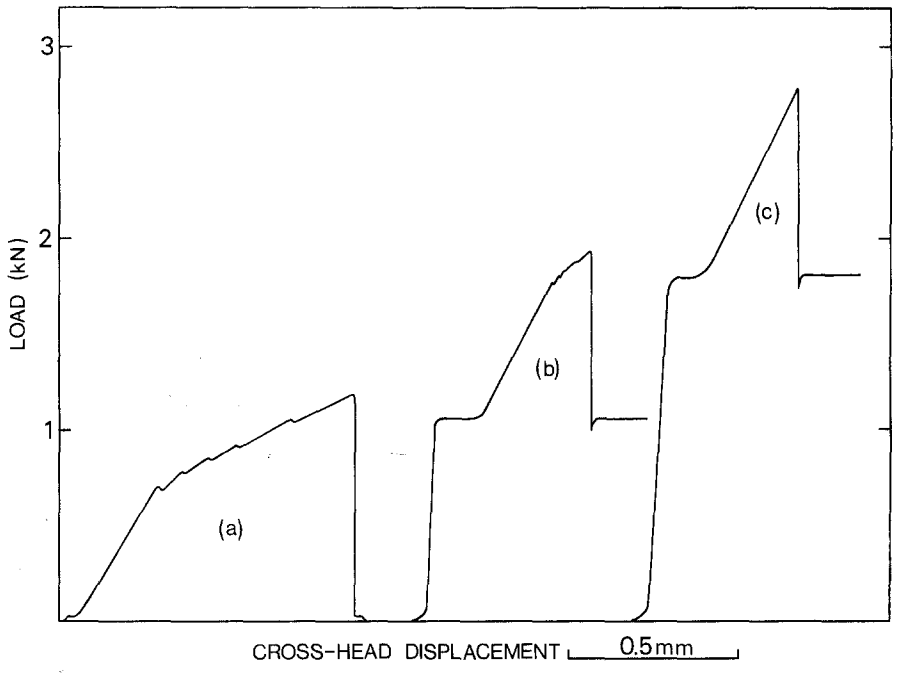

Figure 1 Load–cross-head displacement curves for pultruded CFRP specimens tested (a) at atmospheric pressure and under superposed pressures of (b) 150 and (c) 300 MN m^{-2}. In (b) and (c) the initial load before the horizontal part of the curve is reached is caused by testing assembly friction (approximately constant for each pressure). Note decrease, to zero at 300 MN m^{-2}, in the non-Hookean specimen deflection with increase in pressure.

tensile stress-controlled process requires that the maximum principal stress (specimen applied stress plus hydrostatic pressure) remains constant as H varies. This has in fact been reported for a 56% V_f carbon fibre/nickel composite [8, 9], but no such simple relationship was found in CFRP then studied [9–11]. These latter results, however, indicated that a critical tensile stress model was inapplicable to tensile failure at nearly 1 GN m^{-2} of prototype pultruded 60% V_f CFRP, produced a decade ago [10]. Current commercial CFRP pultrusions are approximately twice as strong in tension [7] and it is with such material that our communication will deal.

2. Experimental procedure

Specimens were machined from ~ 6 mm diameter pultruded rods supplied by Courtaulds Ltd which contained ~ 60% V_f of type A carbon fibres in an epoxy resin matrix. The majority of the specimens tested was of the design illustrated in Fig. 1a of our previous paper [7] and contained no gauge length of constant cross-section. For this investigation the section was reduced, over a length of 10 mm and with a radius of 12.5 mm, to a minimum diameter of 0.8 to 1.0 mm. This ensured tensile failures whilst using the maximum shoulder length (~ 40 mm) that could be accommodated within the limited space available inside the pressure cell. Some complementary atmospheric tests, for which there are fewer geometric constraints, were performed on specimens which contained a 12.5 mm gauge length of ~ 1 mm nominal diameter. Most of these samples were unloaded (before failure) for examination.

All specimens were strained in uniaxial tension on a Hedeby universal tester at a rate of 0.1 mm min^{-1}. The machine was fitted with a Coleraine pressure cell which allows the superposition of pressures of up to 300 MN m^{-2} using "Plexol", a synthetic diester, as a medium. Loads were monitored on a BLH semiconductor load cell and included the frictional forces acting on the loading and dummy rods. These forces could be determined before and after each test and the interpolated value subtracted from the total load at failure, as illustrated in Fig. 1.

The failure surfaces of some specimens were examined on an ISI Super III scanning electron microscope. Other samples were mounted in polyester resin and sectioned and polished parallel to the fibre axis prior to examination on the SEM or a Zeiss Ultraphot II optical microscope. In an attempt to delineate more clearly

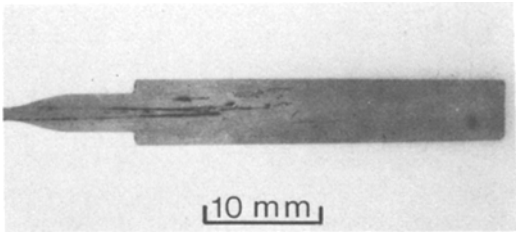

Figure 2 Transverse crack, delineated by a dye penetrant technique as "tram-lines", in a sectioned specimen which had been loaded at atmospheric pressure.

transverse cracks emanating from the minimum cross-section of deformed specimens, several techniques were attempted on mounted and sectioned samples. The use of a "dye penetrant" fluid, as conventionally used with metals, proved quite successful. Once the excess penetrant had been removed, the crack was revealed by spraying the sectioned specimen with a matt, white, cellulose-based paint. This material not only provided a sufficiently absorbent coating to draw the penetrant from the crack, thereby rendering it visible, but was also fine enough to allow the location of the crack tip. This method was more reproducible than either optical and scanning electron microscopic techniques or using a conventional dye penetrant "developer". A transverse crack penetrating the specimen shoulder in a specimen tested at atmospheric pressure is presented in Fig. 2.

Figure 3 Optical micrograph of a section of a tensile specimen with a 12.5 mm gauge length which had been stressed to 1.6 GN m^{-2} at atmospheric pressure and unloaded. Note the broken fibres.

3. Results

The atmospheric tensile strength of our CFRP was found to be 1.99 ± 0.13 GN m^{-2}. A typical load-displacement plot is presented in Fig. 1, which also includes traces for samples tested at 150 and 300 MN m^{-2} superposed pressure. As can be seen from Fig. 1a, a marked departure from Hookean behaviour took place at loads corresponding to applied tensile stress of 1.20 ± 0.04 GN m^{-2} for atmospheric tests. If specimens were strained to below this stress, unloaded and sectioned, no signs of damage associated with the minimum section was detected, (◇ on Fig. 4). Examination of specimens that had been stressed between 1.2 and 1.5 GN m^{-2} revealed interlaminar cracks, such as in Fig. 2 (◈ on Fig. 4), previously described by us as "tram-lines" [7]. Broken fibres could only be detected for minimum section stresses of 1.6 GN m^{-2} and above, e.g. Fig. 3 (◆ on Fig. 4).

The first effect of superposed pressure on the load–deflection response (e.g. Fig. 1b) was to increase the load at which departure from linear deformation took place. The corresponding principal tensile stress increased, approximately linearly, with pressure from its atmospheric value of 1.2 ± 0.04 GN m^{-2} to 1.53 ± 0.05 at 150 MN m^{-2} pressure (Fig. 4). The failure strength concurrently decreased with increasing pressure, from the atmospheric value of 1.99 ± 0.13 to 1.68 ± 0.16 GN m^{-2}.

Examination of sectioned failed samples (by the dye penetrant technique) tested in the pressure region $\leqslant 150$ MN m^{-2} revealed that the extent to which transverse cracking ("tram-lines") extended into the specimen head also decreased with pressure, from 23 to 7 mm (Table I). The appearance of fracture surfaces also changed from "random bundle" [12] at atmospheric pressure to a more localized failure at the minimum cross-section; fractographs illustrating this are presented as Figs. 5a and b and 6a and b.

A marked change in behaviour was observed in

TABLE I The variation with superposed pressure in the length that transverse cracks grow to before tensile failure of pultruded CFRP

Superposed pressure (MN m^{-2})	Crack length (± 3 mm)
Atmospheric	23
50	19
100	12
150	7
200, 250, 300	0

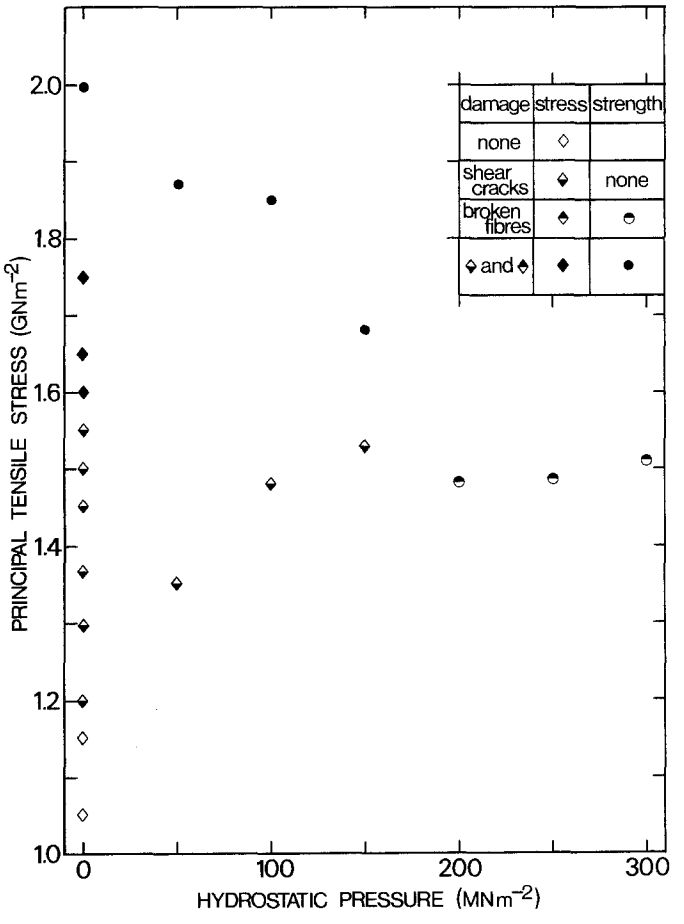

Figure 4 Fracture strengths (●, ◓) of pultruded CFRP specimens tested in tension under superposed pressure. Included also are stress data for the detection of shear cracks (◆) and broken fibres (◆).

all specimens tested at pressures beyond 150 MN m^{-2}. Departures from linear deformation were not detected (Fig. 1c), neither were any transverse cracks associated with the planar fracture surfaces (e.g. Fig. 5c) or found in samples sectioned and examined using the dye penetrant. For the pressure region $\geqslant 150\,MN\,m^{-2}$ failure took place at an approximately constant (principal) tensile stress of $1.5 + 0.2$ and $-0.1\,GN\,m^{-2}$ (Fig. 4). The increasing positive error in these data is due to a superposition of systematic error due to the possibility of pressure decreasing during the tensile test on the random error.

4. Discussion

In our previous communication which considered tensile loading of pultruded CFRP [7] it was pointed out that fibre failure is preceded by transverse cracking or "debonding". This, we have suggested, is the initiation stage of a "three stage failure process" which can be associated with a decrease in the slope of the load–deflection curve. For samples with a reduced gauge diameter this can take place at applied tensile stresses as low as $\sim 1.0\,GN\,m^{-2}$, whereas in specimens of the same material, produced without any machining, at significantly higher stress levels, $\sim 1.5\,GN\,m^{-2}$, which corresponded to approximately 75% of the load carrying capacity. In the current investigation all specimens contained a reduced gauge diameter, and debonding, the formation of cracks parallel to the loading and fibre axis, was observed at atmospheric pressure at a stress of $\sim 1.2\,GN\,m^{-2}$, as indicated in Fig. 3.

This stage, furthermore, appears to be associated with a critical "tensile" rather than "shear" stress. Thus, if the shoulder length (Fig. 1a, [7]) is varied, thereby altering the area over which the shear (but not the normal) stress is calculated, deviations from linear deformation occur at reasonably constant values of tensile stress, whereas the nominal shear stress can vary from 18 ± 2 to $3.5 \pm 0.3\,MN\,m^{-2}$ as the shoulder length is increased from 15 to 75 mm [13]. This is consistent with our hypothesis [7] that debonding occurs as a result of the straightening of fibre bundles (containing prior

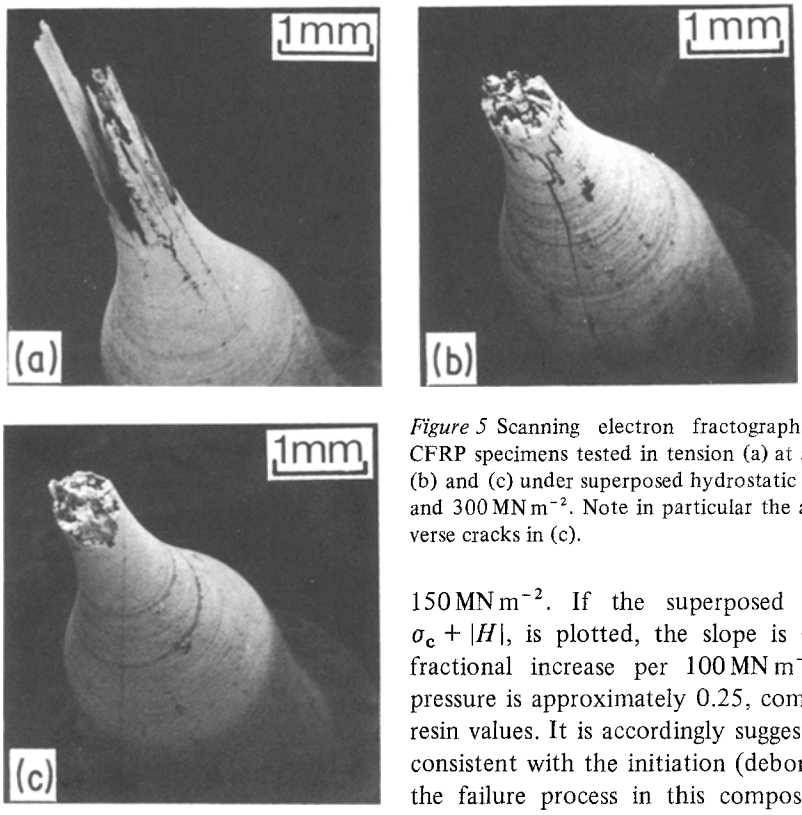

Figure 5 Scanning electron fractographs of pultruded CFRP specimens tested in tension (a) at atmospheric and (b) and (c) under superposed hydrostatic pressures of 150 and 300 MN m^{-2}. Note in particular the absence of transverse cracks in (c).

curvature) against the transverse support of the matrix. Eventually, we have suggested, this is overcome when the transverse tensile strength of the matrix is exceeded locally. If this is the critical mechanism, and debonding is controlled by the properties of the matrix, then the superposition of hydrostatic pressure should influence this stage of the process in the same way as it does the tensile properties of the epoxy resin matrix.

The suggested relation for the critical composite tensile stress for debond initiation [7, 14] at atmospheric pressure is:

$$\sigma_c = \frac{8R\sigma_t}{D} \quad (1)$$

where R is the existing radius of curvature of a fibre bundle of diameter, D, and σ_t is the tensile strength of the matrix. Wronski and Pick [15] have found that for two different epoxy resins the superposed tensile yield strength, $\sigma_t + |H|$, increased with pressure, H, by $-0.19H$. This was equivalent to fractional increases in σ_t of 0.22 and 0.28 per 100 MN m^{-2} superposed pressure [16]. Now, the pressure dependence of the principal stress, σ_c, at which debonding is initiated under pressure, Fig. 4, has a slope of ~ 2.0 for $H <$ 150 MN m^{-2}. If the superposed tensile stress, $\sigma_c + |H|$, is plotted, the slope is ~ 3.0 and the fractional increase per 100 MN m^{-2} superposed pressure is approximately 0.25, comparable to the resin values. It is accordingly suggested that this is consistent with the initiation (debonding) stage of the failure process in this composite being controlled by the "tensile" properties of the epoxy resin matrix alone. The foregoing argument, employing superposed as well as principal stresses, appears necessary as, in general, yielding (of the resin) is related to shear (and therefore superposed) stresses and fracture (of the fibres) to the principal stresses. In Fig. 3 principal stresses only are plotted.

The final stage of this composite failure involves breaking of the fibres. The effect of superposed pressure on the fracture strength of carbon fibres has not been, to the authors' knowledge, investigated directly, but results on a nickel matrix composite, which failed after Hookean deformation [8, 9], indicate that the process takes place at a constant principal tensile stress. So, if the ultimate load carrying capacity of this composite were controlled by fibre strength, the principal stress at failure, σ_t, would be independent of pressure.

For pressures < 150 MN m^{-2}, however, there is, Fig. 4, a significant reduction of σ_t with increasing pressure. To interpret this we consider the second stage of the atmospheric failure process: delamination [7], the "growth" of debonded regions leading to the detachment of surface bundles, before the final "propagation" stage when failure of fibre bundles at separate cross-sections occurs.

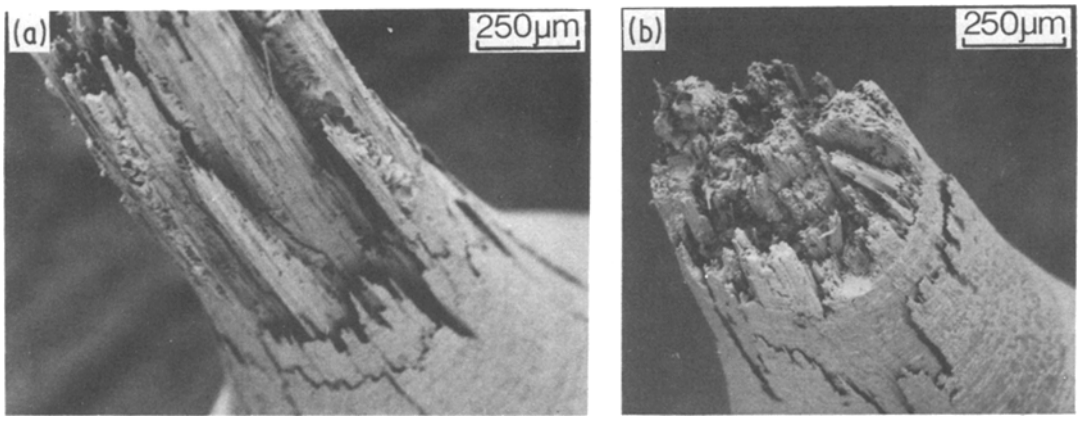

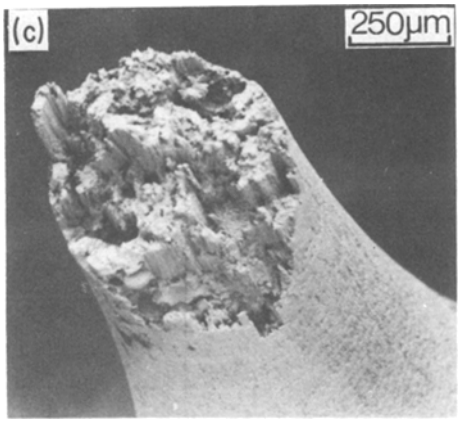

Figure 6 Scanning electron fractographs of the same specimens as for Fig. 5, taken at higher magnifications. Note the reduction in fibre pull-out with increasing hydrostatic pressure.

Delamination takes place under conditions of increasing load and it has been suggested [7] that the straightening of detached surface bundles, which, because of the prior curvature, were incapable of being fully loaded, enables the composite to support additional loads (Figs. 1a and b), until numerous fibre failures occur. Superposition of hydrostatic, and therefore transverse, pressure can only make transverse cracking more difficult. It is also suggested that a significant effect of delamination is to isolate fibre bundles from each other, rendering the first fibre fractures that occur within them, as a result of the normal statistical distribution of fibre strengths, less damaging to the composite. Thus, as debonding, delamination and load redistribution become more difficult with increasing pressure, the ultimate load carrying capacity of the composite can decrease: σ_t for $H < 150\,\mathrm{MN\,m^{-2}}$ in Fig. 4.

The principal stress at fracture decreases to $\sim 1.5\,\mathrm{GN\,m^{-2}}$. It is to be noted that in interrupted atmospheric tests (Fig. 4) broken fibres were detected in samples that had been stressed to $\geqslant 1.6\,\mathrm{GN\,m^{-2}}$, and it is suggested that these stresses are sufficiently close to be associated with the same mechanism. For tests at pressures exceeding $150\,\mathrm{MN\,m^{-2}}$ there was no evidence of debonding or delamination preceding failure. At the higher pressures, we would thus suggest, there is no isolation of fibre bundles and less scope for load redistribution. The first fibre fractures, which appear to occur at a similar principal stress as at atmospheric pressure, can be free to propagate throughout the specimen cross-section, an example of the classical case treated by Kelly and Davies [17]. The relatively flat fracture surfaces shown by samples tested in this pressure range (Figs. 5 and 6) support this interpretation. The variation in strength is lower than for atmospheric composite tests and similar to that for tests of fibres rather than composites [18, 19]. These results are the only ones that can be interpreted solely in terms of fibre properties; when the critical (principal) tensile stress in the fibres, independent of pressure, is reached, tensile failure results.

The data clearly show that, as in axial compression [16, 20], in axial tension the resin properties can not be neglected in relation to the strength of a real fibrous composite. Only when stress redistribution between bundles is suppressed, i.e. above $150\,\mathrm{MN\,m^{-2}}$ pressure for our CFRP, is the composite strength solely dependent on the relevant fibre strength. This behaviour somewhat resembles that of a nickel matrix composite [8, 9], though the micromechanics of its failure process were probably different.

The $H < 150\,\mathrm{MN\,m^{-2}}$ results support our model of composite failure which invokes a three-

stage process. The resin strength-controlled debonding process is clearly important in relation to fatigue and environmental properties. Strengthening the matrix, for the same fibre bundle curvature, should increase σ_c. No simple fibre property dependent mechanism can account for the σ–H behaviour for $H < 150\,\mathrm{MN\,m^{-2}}$.

The enhanced difficulty of debond propagation leads to fibre fractures, within smaller delamination lengths. The combination of this and increased difficulty of load redistribution between bundles results in lower strength and failure within a smaller longitudinal section. When no debonding precedes initial fibre failures, these result in catastrophic cracking at $\sim 1.5\,\mathrm{GN\,m^{-2}}$.

Acknowledgement

The authors wish to acknowledge the support of the Science and Engineering Research Council.

References

1. M. FUWA, A. R. BUNSELL and B. HARRIS, *J. Mater. Sci.* **10** (1975) 2062.
2. M. FUWA, B. HARRIS and A. R. BUNSELL, *J. Phys. D.* 8 (1975) 1460.
3. A. R. BUNSELL and D. VALENTIN, *Compos. Struct.* **1** (1983) 67.
4. C. ZWEBEN and B. W. ROSEN, *J. Mech. Phys. Solids* 18 (1970) 189.
5. D. G. HARLOW and S. L. PHOENIX, *J. Compos. Mater.* 12 (1978) 195.
6. B. W. ROSEN, *Amer. Inst. Aeronaut. Astronaut. J.* 2 (1964) 1985.
7. A. S. WRONSKI and T. V. PARRY, *J. Mater. Sci.* 19 (1984) 3421.
8. B. R. WATSON-ADAMS, J. J. DIBB and A. S. WRONSKI, Metal Matrix Composite Materials, November 1972, Liverpool Polytechnic Symposium, edited by R. W. Jones, paper 4.
9. A. S. WRONSKI, Proceedings of the Third International Conference on Fracture, Munich, 1973, II–332.
10. J. J. DIBB, PhD thesis, University of Bradford (1975).
11. J. J. DIBB, A. S. WRONSKI and B. R. WATSON-ADAMS, *Composites* 4 (1973) 227.
12. R. L. McCULLOUGH, "Concepts of Fibre-Resin Composites" (Marcel Dekker, New York, 1971) p. 46.
13. A. CUCKSON, Materials Science Undergraduate Project Report, University of Bradford (1983).
14. D. G. SWIFT, *J. Phys. D.* 8 (1975) 223.
15. A. S. WRONSKI and M. PICK, *J. Mater. Sci.* 12 (1977) 28.
16. A. S. WRONSKI and T. V. PARRY, *ibid.* 17 (1982) 3656.
17. A. KELLY and G. J. DAVIES, *Metall. Rev.* 10 (1965) 1.
18. J. W. HITCHON, W. H. McCAUSLAND and D. C. PHILLIPS, AERE Report R8217 (1975).
19. J. W. HITCHON and D. C. PHILLIPS, AERE Report R9132 (1978).
20. T. V. PARRY and A. S. WRONSKI, *J. Mater Sci.* 17 (1982) 893.

Received 16 July
and accepted 31 July 1984